Available online at www.sciencedirect.com
SCIENCE DIRECT®
ELSEVIER
Journal of Magnetism and Magnetic Materials 263 (2003) 324–331
Journal of magnetism and magnetic materials
www.elsevier.com/locate/jmmm

Monte Carlo and spin dynamics simulation of the fully frustrated anisotropic two-dimensional Heisenberg model

A.B. Lima*, B.V. Costa

Departamento de Física, Campus Pampulha ICEX, Universidade Federal de Minas Gerais, Caixa Postal 702, 30123-970 Belo Horizonte - MG, Brazil

Received 20 November 2002; received in revised form 10 January 2003

Abstract

Using Monte Carlo and spin dynamics techniques we investigate the critical behavior of the classical three component anisotropic Heisenberg model in two dimensions in square lattices of size up to 256^2. We have found that the model has two transitions, as in the two-component planar rotator model, a Kosterliz–Thouless transition at $T_{KT} = 0.3655(5)$ and an Ising transition at $T_I = 0.3690(3)$. Also, we performed preliminary calculations in small lattices in order to obtain the neutron scattering correlation function $S(\vec{q}, \omega)$.

PACS: 64.40.Cm; 75.10.Hr; 75.40.Mg

Keywords: Frustrated; Heisenberg

1. Introduction

Frustrated spin models were the subjects of several works since the concept was introduced in connection with spin glasses and fully frustrated models [1,2]. The latter has been studied extensively as a model for 2D coupled arrays of Josephson junction and superconducting wires in a transverse magnetic field [3–5]. Of particular interest is the fully frustrated planar rotor (FFPR) in two-dimensions. To the contrary of the unfrustrated model which cannot present long-range order at any finite temperature [6], the FFPR is expected to display a richer critical behavior due to two different symmetries. Beside the spin $U(1)$ symmetry it has a Z_2 discrete symmetry which leads to the possibility of long-range order. The FFPR model is defined as

$$H = \sum_{\langle i,j \rangle} J_{i,j} \vec{S}_i \cdot \vec{S}_j \tag{1}$$

or

$$H = \sum_{\langle i,j \rangle} J_{i,j} \cos(\theta_i - \theta_j), \tag{2}$$

where i and j enumerate lattice sites, $\vec{S}_i = |\vec{S}|\{\cos\theta_i, \sin\theta_i\}$ is a two-dimensional vector, θ_i is the angle at the lattice point i and $J_{i,j}$ is an

*Corresponding author. Tel.: +553134995648; fax: +553134995600.
E-mail address: alima@fisica.ufmg.br (A.B. Lima).

0304-8853/03/$ - see front matter
doi:10.1016/S0304-8853(03)00105-7

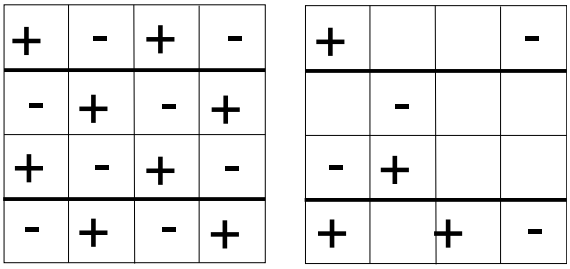

Fig. 1. Diagram of the square lattice showing the ferromagnetic (thin lines) and antiferromagnetic (double lines) couplings $J_{i,j}$. The symbols + and − represent vortices and antivortices. The figure at the left and right hand sides are for $T = 0$ and $T > 0$, respectively.

exchange coupling which is ferromagnetic in all lines in the x direction and is alternately ferromagnetic and anti-ferromagnetic in the y direction as shown in Fig. 1. The coupling distribution leads the FFPR model to have a checkerboard pattern of plaquetes with positive or negative chirality in the ground state

$$f = \frac{1}{\pi} \sum_{\text{plaquete}} (\theta_i - \theta_j) = \pm 1. \tag{3}$$

In a series of papers Olsson [7] has shown that this model undergoes two phase transitions, one of the Berezinskii–Kosterlitz–Thouless (BTK) [11,12] type, associated to the $U(1)$ symmetry and an Ising transition associated to the discrete Z_2 symmetry due to the f degrees of freedom. He found $T_{\text{BKT}} = 0.446J$ and $T_{\text{I}} = 0.452J$, respectively and the correlation length exponent was found to be consistent with the two-dimensional Ising value $v = 1$. In this report we investigate the fully frustrated anisotropic three-component XY (FFXY) model which has the same symmetry as the FFPR, using numerical techniques. The model is defined as

$$H = \sum_{\langle i,j \rangle} J_{i,j} \vec{S}_i \cdot \vec{S}_j + A \sum_{\langle i,j \rangle} S_i^z S_j^z, \tag{4}$$

where $\vec{S}_i = |\vec{S}|\{\sin\theta_i \cos\phi_i, \sin\theta_i \sin\phi_i, \cos\theta_i\}$ is a spin vector at site i and $A > 0$ (in this work we use $A = |J_{i,j}|$n). Observe that in this model the spin vector has three degrees of freedom in contrast with the one defined by Eq. (1) where the spin vector has two degrees of freedom. Due to the easy plane anisotropy, A, the Heisenberg symmetry is broken leading the system to have the same symmetry as the FFPR model, however, in the FFXY we expect the transition temperatures T_{BKT} and T_{I} to approach each other due to the new degree of freedom introduced. Having this in mind we have performed a very careful Monte Carlo simulation of the FFXY model. To test our program we have used the FFPR model as a test since we can compare them to Olsson's results. We have also performed some preliminary calculation of the spin dynamics for the model obtaining the neutron scattering function $S(\vec{q}, \omega)$ for temperatures above, below and in between T_{BKT} and T_{I}.

2. Background

It is well known that the BKT phase transition is driven by the presence of vortices in two-dimensional models with continuous symmetry. In short the BKT picture of the phase transition is as follows. At low temperature spin waves are the relevant excitations of the system. Spin–spin correlation functions fall off slowly with distance, free vortices do not exist but pairs are strongly bound. Vortices pairs cannot disorder the system significantly since they affect only close spins. As the temperature is raised, the distance between vortex–antivortex pairs grows up to T_{BKT}. Then, free vortices exist, the system is disordered and the spin–spin correlation function falls exponentially. In the fully frustrated models the vortex density at $T = 0$ is $\rho_{\text{v}} = 1$. Vortex-antivortex pairs are distributed over the lattice as in a checkerboard (see Fig. 1). Once the temperature is raised they begin to annihilate each other until ρ_{v} reaches some critical value $\rho_{\text{v}} = \rho_{\text{TKT}}$ when pairs start to unbind and we have a BKT transition. At this temperature the vortex density is high enough, so that, an infinite cluster of vortices still exists in the system and the Ising symmetry is preserved. As the temperature increases the density goes below a second critical value $\rho_{\text{v}} = \rho_{\text{I}}$ where the Ising order is lost. The precise determination of the temperature for a BKT transition is a difficult task due to absence of sharp peaks in the thermodynamic quantities. One way to extract T_{BKT} was suggested

by Weber and Minnhagen [8] by calculating the helicity modulus defined as

$$\Upsilon = \frac{\partial^2 F}{\partial \Delta^2}, \tag{5}$$

where Δ is a small twist across the system in one direction. The finite size scaling for the helicity modulus is given by the Weber and Minnhagen's relation

$$\frac{\Upsilon_L \pi}{2T_{BKT}} = 1 + \frac{1}{2(\ln L + l_0)}, \tag{6}$$

where l_0 is a parameter to be determined. Some care must be taken in using this relation, since the scaling relation is obeyed only for large lattices. To study the Z_2 transition it is customary to define the staggered magnetization

$$M_I = \frac{1}{L^2}\left|\sum_{\vec{r}} m(\vec{r})(-1)^{x+y}\right|. \tag{7}$$

According to the scaling hypothesis

$$M_I \approx L^{-\beta/\nu} f\left(tL^{1/\nu}\right). \tag{8}$$

The magnetic susceptibility χ_I has the following scaling law:

$$\chi_I = \frac{L^2}{k_B T}\langle M^2\rangle - \langle M\rangle^2 \approx g_0 L^{-\gamma/\nu}. \tag{9}$$

In the above equations $t = (T - T_I)/T_I$. We can use the hyperscaling relation in two-dimensions, $2\nu = \gamma + 2\beta$, to calculate T_I, β/ν and γ/ν. The critical exponent ν is calculated through the specific heat behavior

$$C_{max} \approx L^{-\alpha/\nu}, \tag{10}$$

and the hyperscaling relation $\alpha = 2 - 2\nu$. We have also calculated the Binder cumulant

$$U = 1 - \frac{\langle M^4\rangle}{3\langle M^2\rangle^2}, \tag{11}$$

which is independent of the lattice size L at the critical point, $U_L = U^*$ for sufficiently large lattices. For a more complete discussion see Ref. [7] and references therein.

3. Simulation Details

Our simulations were carried out using the standard Metropolis algorithm combined with overrelaxation updates [9]. We have used lattices of size $L \times L$ and periodic boundary conditions with $L = 8, 16, 32, 64, 128$ and 256 for the FFPR and $L = 20, 40, 60, 80$ and 160 for the FFXY models, respectively. As discussed before, we have used the FFPR as a test for our program. Since we knew in advance the region to search in the FFPR model we focused there our attention, performing the simulation inside the temperature region $0.400 \leqslant T \leqslant 0.500$ with step sizes of $\Delta T = 0.01$. In order to reach thermodynamical equilibrium we performed long runs of size $100 \times L \times L$ which seemed to be enough to equilibrate the system. After this procedure we started to store the energy and magnetization values separated by 5 MC steps to break correlation between successive configurations. For $L = 8, 16, 32$ and $L = 64$ we stored 4×10^6 values and 10^6 values for $L = 128$ and $L = 256$. Then, we have used the single histogram technique [10] to study the interesting regions of temperature. In our simulations, when not indicated, the error bars are smaller than the symbols. For the FFXY model, large fluctuations are present due to the extra degree of freedom, so that, we had to perform 4×10^6 for all lattice sizes in order to get reasonable error bars.

4. Results

In this section we present and analyze our results for both, the FFPR and FFXY models.

4.1. FFPR model

4.1.1. Z_2 transition

First we analyze the staggered magnetization as a function of the system size L. We plot several values of $\ln M$ as a function of $\ln L$ for fixed temperatures T^* adjusting a straight line to each set point as given by the finite size scaling relations. Using the best adjust and Eq. (8) we extract $T_I^M = 0.4505\,J(5)$ and $\beta/\nu = 0.123(7)$ as shown in Fig. 2. In Fig. 3 we show the Binder

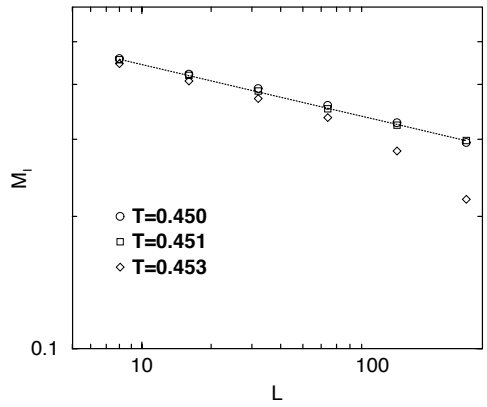

Fig. 2. Magnetization M_I for lattice sizes $L = 8, 16, 32, 64, 128, 256$ for three temperatures. The doted line is a χ^2 fit.

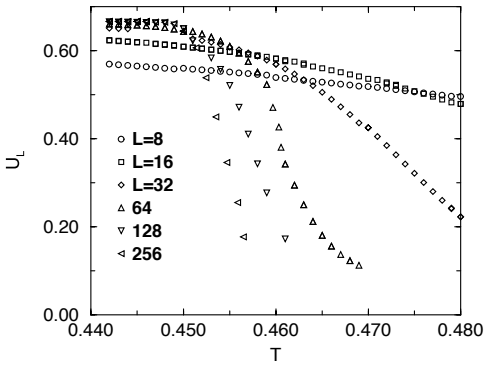

Fig. 3. The Binder cumulant as a function of temperature for several lattice sizes.

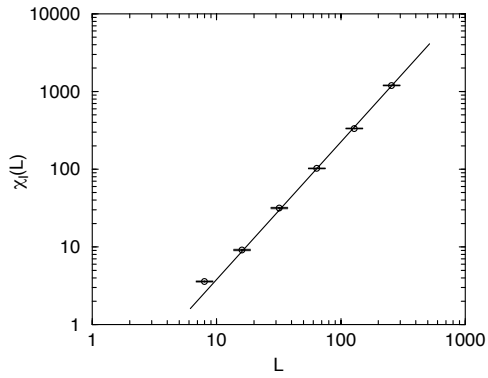

Fig. 4. Maxima of the susceptibility as a function of L. The straight line is the best χ^2 fit which gives $\gamma/\nu = 1.746(30)$.

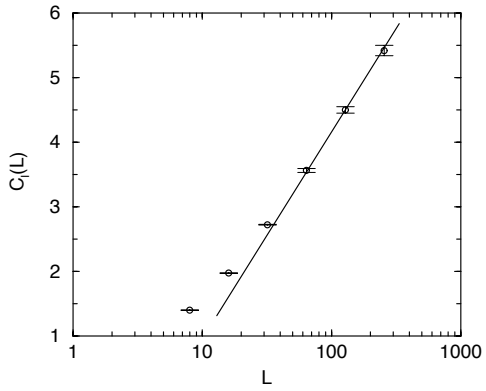

Fig. 5. Maxima of the specific heat as a function of L. The straight line is the best χ^2 fit, showing the Ising behavior $\alpha = 0$.

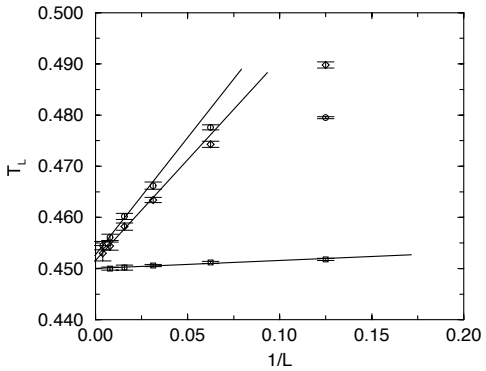

Fig. 6. Binder cumulant intersections (squares), temperature at the maxima of the specific heat (diamonds) and the temperature at the Z_2 susceptibilities (circles). The straight lines are the best fittings for $L > 32$.

cumulant as a function of temperature and lattice size. There is no unique crossing point independent of the systems size if we consider the smaller lattices. However, for sufficiently large $L \geqslant 64$ we observe that all lines cross at the same point U^*. The exponent relation γ/ν is obtained from the plot of the logarithm of the maxim of the susceptibility χ_I as a function of $\ln L$ as shown in Fig. 4. The best fit to the points, excluding $L = 8, 16$ gives $\gamma/\nu = 1.746(30)$. In order to get the critical exponent α we plot the maxima of the specific heat as a function of L in Fig. 5 in a semi-log scale. The specific heat is dominated by the leading singularity and has a Ising behavior, $\alpha = 0$.

Using the hyperscaling relation for α we obtain $\nu = 1$. The critical temperature T_I is obtained by plotting the temperature where the susceptibility is maximum and the crossing temperatures of the binder cumulants in a same plot as a function of $1/L^{\nu}$ as shown in Fig. 6. In the same figure is also shown the maximum of the specific heat. It converges to the same point as the susceptibility and cumulant inside the error bars. From this plot we get $T_I = 0.4511J(10)$.

4.1.2. $U(1)$ transition

In order to determine the BKT transition temperature we measured the helicity modulus and the susceptibility χ_{BKT}. In Fig. 7 we plot the intersection temperatures between the universal jump line $(2/\pi)T$ and the helicity modulus Υ which gives an upper bound, T_{BKT}^{upper}, for T_{BKT}. On the basis of this analysis we conclude that $T_{BKT}^{upper} = 0.4463J(3)$. To obtain T_{BKT} we solve Eq. (6) for $\ln L$ and plot the resulting quantities as a function of $\ln L$. At T_{BKT} we expect a straight line. In Fig. 8 we show some results using this procedure, which gives $T_{BKT} = 0.4410J(5)$, even considering the error bars it is far below T_{BKT}^{upper} obtained using the universal jump criterion.

Our results are essentially the same as those obtained by Olsson confirming that our code is correct. We are now ready to proceed to the XY model.

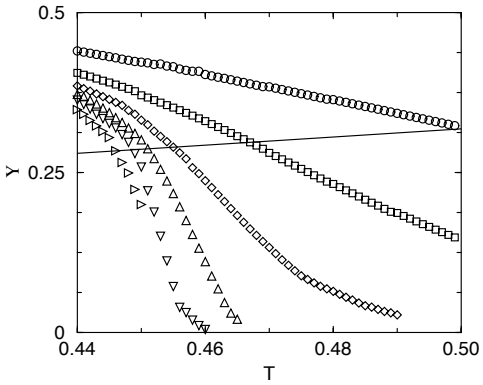

Fig. 7. Spin helicity modulus as a function of T. Each intersection with the line $(2/\pi)T$ gives an upper bound of the BKT transition temperature.

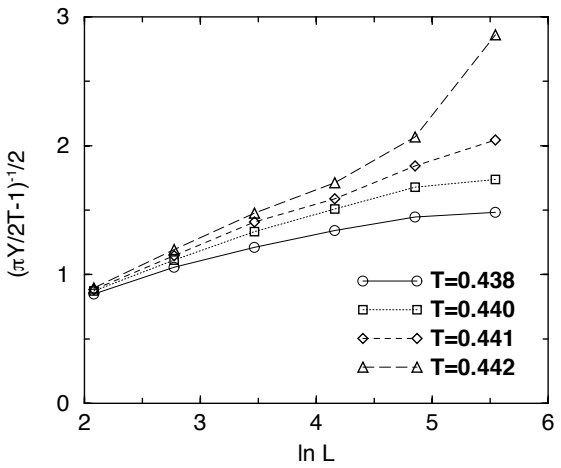

Fig. 8. Helicity modulus plotted as a function of $\ln L$. At the BKT transition and large L limit the points must define a straight line.

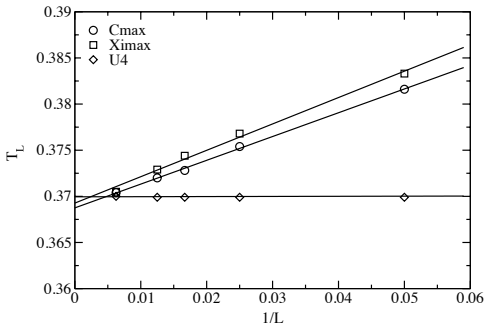

Fig. 9. Binder cumulant intersections (diamonds), temperature at the specific heat maxima (circles) and the temperature at the Z_2 susceptibilities maxima (squares). The straight lines are best fittings for $L > 32$.

4.2. XY model

Now, once we have checked our code we can study the FFXY doing a close analysis as the one for the FFPR model above.

4.2.1. Z_2 transition

In Fig. 9 we show the maxima of the susceptibility, Binder's cumulant and maxima of the specific heat for $L = 20, 40, 60, 80$ and 160. Extrapolation of $L \to \infty$ using these three quantities gives $T_I = 0.3690J(3)$. The critical exponent γ is

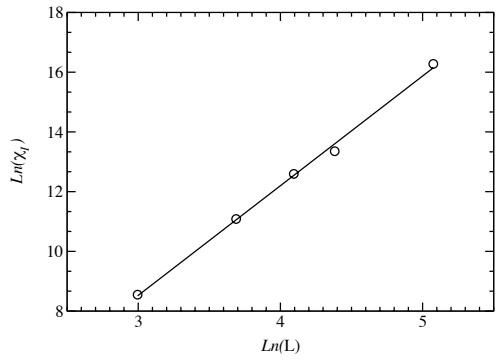

Fig. 10. Maxima of the Z_2 susceptibilities. The straight lines are best fittings for $L > 32$ which gives $\gamma/\nu = 1.67(9)$.

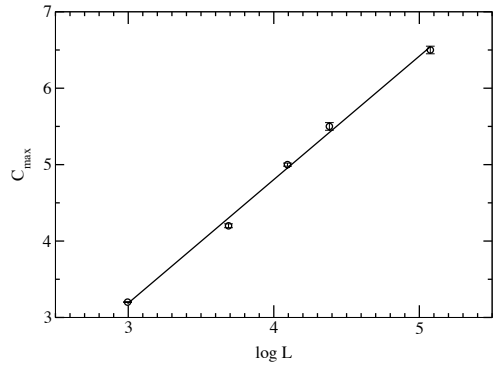

Fig. 11. Maxima of the specific heat as a function of the lattice size. For the XY model the straight line is the best fitting.

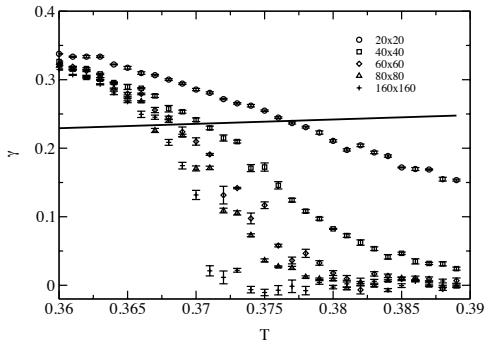

Fig. 12. Helicity as a function of temperature for the XY model. The straight line is $(2/\pi)T$.

obtained as $\gamma = 1.67(0.9)$ with the specific heat having an Ising behavior as in the FFPR, as shown in Figs. 10 and 11, respectively.

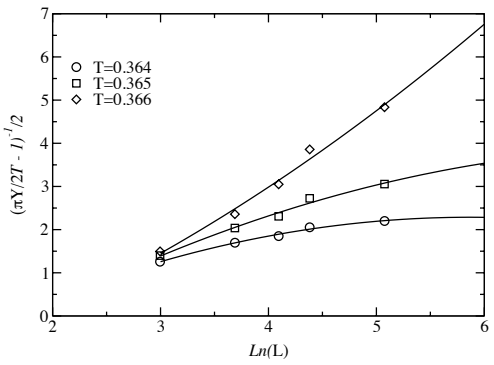

Fig. 13. Helicity modulus as a function of ln L.

4.2.2. $U(1)$ *transition*

As before we estimate an upper bound for the BKT transition $T_{\mathrm{BKT}}^{\mathrm{upper}}$ by collecting the intersection temperatures between the universal jump line $(2/\pi)T$ and the helicity modulus Υ which gives $T_{\mathrm{BKT}}^{\mathrm{upper}} = 0.3665J(5)$ (Figs. 12 and 13). Following the analysis for the FFPR model we obtain $T_{\mathrm{BKT}} = 0.3655J(5)$, which matches $T_{\mathrm{BKT}}^{\mathrm{upper}}$ if we use the largest error bars. Following Minnhagen's work, it may indicate the presence of a universal jump for this model. However, due to the large error bars, more work has to be done in this subject in order to make this point clear.

5. Dynamics

In this section we present a preliminary calculation of the dynamical neutron scattering function $S(\vec{q},\omega)$ for the FFXY model which is an experimental observable and is fundamental for the study of the spin dynamics. It is defined for momentum transfer $\vec{q}$ and frequency transfer ω as the space–time Fourier transform

$$S^{\alpha\alpha}(\vec{q},\omega) = \sum_{\vec{r},\vec{r}'} \int_{-\infty}^{+\infty} \mathrm{e}^{\mathrm{i}\omega t} C^{\alpha\alpha}(\vec{r}-\vec{r}',t)\frac{dt}{2\pi}, \qquad (12)$$

of the space-displaced, time-displaced spin–spin correlation function

$$C^{\alpha\alpha}(\vec{r}-\vec{r}',t) = \langle S^{\alpha}_{\vec{r}}(t) S^{\alpha}_{\vec{r}'}(t')\rangle, \qquad (13)$$

where $\alpha = x,y,z$ is the spin component, the displacement $\vec{r}$ is measured in units of the lattice

spacing, and the brackets $\langle \cdots \rangle$ denote the thermal ensemble average. As far as we know there are no previous analytical or numerical results for the dynamics of this model. The equations of motion for each spin is

$$\frac{d\vec{S}_i}{dt} = \vec{S}_i \times H_{\text{eff}}, \tag{14}$$

$$H_{\text{eff}} = \sum_{\alpha} J_{i,j}(S^{\alpha}_{i-1,j} + S^{\alpha}_{i,j-1} + S^{\alpha}_{i+1,j} + S^{\alpha}_{i,j+1})\hat{e}_{\alpha}, \tag{15}$$

where α stands for x, y, z. Eq. (14) represents a set of coupled equation to be integrated numerically. To integrate the equations of motion we have used a fourth-order Runge–Kutta scheme with size step of $\delta t = 0.02J^{-1}$ We performed the simulation for four temperatures, $T = 0.2J, 0.3655J, 0.369J$ and $0.4J$ using lattices of sizes $L = 40$ and 60. Equilibrium configurations were created at each temperature using the Metropolis Monte Carlo method. Between 500 and 1000 equilibrium configurations were generated for each size and temperature. We found that this many configurations were necessary to sufficiently reduce the statistical errors in the resulting scattering function.

Starting with each equilibrium configuration, the time dependence of the spins were determined. The maximum integration time was $t_{\max} = 20J^{-1}$. The results for different values of L were very close and we used $L = 40$ considering that this is a preliminary calculation. Also, in order to reduce

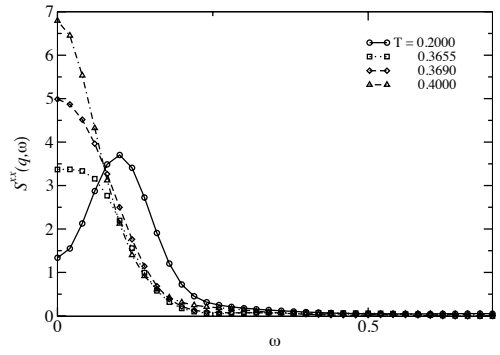

Fig. 14. Temperature dependence of the xx component of the neutron scattering function $S(q,\omega)$ as a function of frequency ω. Lattice size $L = 40$ and momentum $q = 2\pi/40$ in all cases.

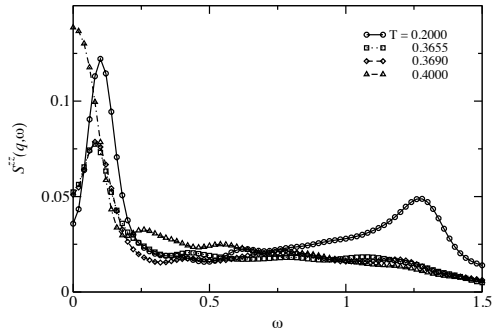

Fig. 15. The same is in Fig. 14 for the zz component of the neutron scattering function.

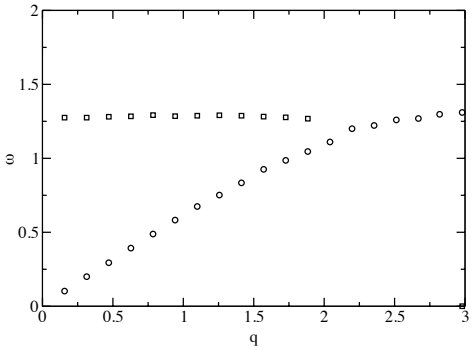

Fig. 16. Dispersion relation for S^{zz}. There is an optical and an acoustic mode. Lattice size is $L = 40$ and the temperature is $T = 0.2000J$.

memory and CPU time, we restricted ourselves to moment $\vec{q} = (q, 0)$ and $(0, q)$, with q determined by periodic boundary conditions

$$q = n_q \frac{2\pi}{L}, \quad n_q = 1, 2, \ldots, L. \tag{16}$$

The frequency resolution $\Delta\omega$ is determined by the maximum time of integration which introduce oscillations of period $2\pi/t_{\max}$ into $S^{\alpha\alpha}(\vec{q},\omega)$. To smoothen the oscillations, we use a frequency resolution function, replacing

$$C^{\alpha\alpha}(\vec{r} - \vec{r}', t) \quad \text{by} \quad C^{\alpha\alpha}(\vec{r} - \vec{r}', t)\exp\left(-\tfrac{1}{2}(t\delta\omega)^2\right). \tag{17}$$

In Figs. 14 and 15 we show $S^{xx}(\vec{q},\omega)$ and $S^{zz}(\vec{q},\omega)$ for four different temperatures, below, above and at the critical temperatures. For the in plane correlation is almost impossible to identify the small oscillation peaks probably due to the

revolution function which smoothes the $S(\vec{q},\omega)$ waves. For the out of plane correlation, we observe well-defined small oscillation peaks as shown in Fig. 16. There are two magnon branches since the model has a cell with ferro and antiferromagnetic couplings. Although this is a preliminary calculation it seems that the model has a very rich dynamical structure which will be the subject of a future work.

6. Conclusion

We performed careful simulation for the fully frustrated planar rotator and XY models in two-dimensions. For the planar rotator our results confirm those from Olsson: The planar rotator model has two transitions, coming from low temperature it has an Ising transition then it undergoes a BKT transition. The distance between the transition temperature is about 2%. The specific heat has an Ising behavior and there is no universal jump in the helicity modulus. For the XY model, the question is a bit more difficult to respond than in the FFPR since the extra degree of freedom introduced by the z component of the spins. Considering that both models are in the same universality class we found that the two critical temperatures, T_{BKT} and T_{I}, are less than 1% apart. We have also done some preliminary calculation on the dynamics of the model. Our preliminary calculation shows a rich dynamical structure that will be explored in a future work.

Acknowledgements

This work was partially supported by CNPq and FAPEMIG (Brazilian agencies). Numerical work was done in the LINUX parallel cluster at the Laboratório de Simulação Departamento de Física - UFMG.

References

[1] J. Villan, J. Phys. C 10 (1977) 4793.
[2] E. Fradkin, B. Huberman, S.H. Shenker, Phys. Rev. B 18 (1978) 4789.
[3] B.I. Halperin, D.R. Nelson, J. Low Temp. Phys. 36 (1979) 599.
[4] S. Teitel, C. Jayaprakash, Phys. Rev. Lett. 51 (1983) 1999.
[5] P. Minnhagen, G.G. Warren, Phys. Rev. B 24 (1981) 2526.
[6] N.D. Mermin, H. Wagner, Phys. Rev. Lett. 17 (1966) 1133.
[7] P. Olsson, Phys. Rev. Lett. 73 (1994) 3339;
P. Olsson, Phys. Rev. B 52 (1995) 4526;
P. Olsson, Phys. Rev. B 77 (1996) 4850;
P. Olsson, Phys. Rev. B 55 (1997) 3585.
[8] H. Weber, P. Minnhagen, Phys. Rev. B 38 (1988) 8730.
[9] F.R. Brown, T.J. Woch, Phys. Rev. Lett. 58 (1987) 2394.
[10] A.M. Ferrenberg, R.H. Swendsen, Phys. Rev. Lett. 61 (1998) 2635.
[11] V.L. Berezinskii, Zh. Eksp. Teor. Fiz. 61 (1971) 1144.
[12] J.M. Kosterlitz, D.J. Thouless, J. Phys. C 6 (1973) 1181.